Downregulation of MGST3 promotes colorectal cancer progression

YUCHUN WU[1,2], CHANGJIANG FAN[1], JIAQI ZHOU[2], FENGSHAN HUANG[1,2], YANG ZHANG[2], YUQI HE[3] and JIANXUN WANG[1]

[1]Department of Pathology and Pathophysiology, School of Basic Medicine, Qingdao University, Qingdao, Shandong 266071, P.R. China; [2]Guangdong Provincial Key Laboratory of Synthetic Genomics, Key Laboratory of Quantitative Synthetic Biology, Shenzhen Institute of Synthetic Biology, Shenzhen Institutes of Advanced Technology, Chinese Academy of Sciences, Shenzhen, Guangdong 518055, P.R. China; [3]Department of Gastroenterology, The Seventh Medical Center of Chinese PLA General Hospital, Beijing 100853, P.R. China

Received August 3, 2025; Accepted November 24, 2025

DOI: 10.3892/mco.2026.2938

Abstract. Colorectal cancer (CRC), the third most common malignancy worldwide, presents significant treatment challenges due to an incomplete understanding of its molecular progression. Therefore, identifying the specific developmental mechanisms of CRC holds potential to improve diagnosis, treatment and prognosis. In the present study, RNA-sequencing analysis of samples from patients with an early-stage tumor, advanced carcinoma or adenoma was conducted with the aim of uncovering differentially expressed genes. At the same time, gene knockdown and tumor-related phenotype verification were conducted using a normal colon epithelial cell line. Subsequently, a group of genes related to the target gene was analyzed using The Cancer Genome Atlas (TCGA) database and the differences in colon tumor mutation burden, immune infiltration, epithelial-mesenchymal transition (EMT) and ferroptosis were observed between samples with high and low expression of the gene group. Microsomal glutathione S-transferase 3 (MGST3) was identified as a crucial tumor-suppressive gene in colon cancer pathogenesis. Functional studies demonstrated that MGST3 knockdown in normal human colonic epithelial cells activated glutathione metabolic pathways and induced tumorigenic transformation, characterized by accelerated proliferation and suppression of EMT. TCGA database analysis revealed distinct phenotypes associated with low MGST3 expression, including elevated tumor mutational burden, attenuated EMT processes, diminished immune cell infiltration and enhanced ferroptosis. These findings establish MGST3 as a potential novel regulator of colon carcinogenesis, with its downregulation creating a tumor microenvironment conducive to ferroptosis while simultaneously suppressing EMT and immune responses. The present study not only elucidates previously unrecognized mechanisms driving colon cancer progression but also identifies MGST3-related pathways as promising therapeutic targets for intervention.

Correspondence to: Professor Jianxun Wang, Department of Pathology and Pathophysiology, School of Basic Medicine, Qingdao University, 308 Ningxia Road, Shinan, Qingdao, Shandong 266071, P.R. China
E-mail: wangjx@qdu.edu.cn

Professor Yuqi He, Department of Gastroenterology, The Seventh Medical Center of Chinese PLA General Hospital, 5 Nanmencang, Dongcheng, Beijing 100853, P.R. China
E-mail: chinaendohe@163.com

Abbreviations: CRC, colorectal cancer; EMT, epithelial-mesenchymal transition; MGST, microsomal GST; GST, glutathione S-transferase; KEGG, Kyoto Encyclopedia of Genes and Genomes; TME, tumor microenvironment; PPI, protein-protein interaction; TMB, tumor mutational burden; ROS, reactive oxygen species; GSEA, Gene Set Enrichment Analysis; ICIs, immune checkpoint inhibitors

Key words: CRC, ferroptosis, glutathione metabolism, differential genes, MGST3

Introduction

Colorectal cancer (CRC), the second leading cause of global cancer-related death and the third most common cancer worldwide, exhibits a concerning rise in incidence among younger populations in mainland China, with an annual increase of 1-2% in individuals <55 years (1,2). Although pathological stage at diagnosis remains the strongest prognostic factor, >50% of patients present with advanced or intermediate-stage disease (3), underscoring the urgent need to elucidate CRC pathogenesis for early detection and improved therapies.

CRC primarily arises from adenomatous colonic polyps, the most prevalent type, constituting 60-70% of all colonic polyps. Conventional adenomatous polyps are histologically classified as tubular, villous or tubulovillous. Over time, some adenomas may progress from low-grade dysplasia to high-grade dysplasia, carcinoma *in situ* or invasive adenocarcinoma, with <90% of CRC cases being adenocarcinoma of colonic/rectal mucosal origin (4). Furthermore, 70-90% of CRC cases develop into carcinoma from adenoma, driven by mutations in tumor suppressor genes such as Adenomatous polyposis coli and *TP53* as well as in oncogenes such as *KRAS*,

while a distinct subset (~10%) follows the serrated neoplasia pathway, marked by epigenetic dysregulation (such as *MLH1* promoter hypermethylation) and DNA repair defects (5).

Microsomal glutathione S-transferase (MGST) belongs to the microsomal subfamily of the glutathione S-transferase (GST) family and plays a pivotal role in cellular detoxification (6). Specifically, it catalyzes the conjugation of reduced glutathione to xenobiotic substrates, thereby protecting cells against oxidative stress-induced damage. Furthermore, these enzymes effectively neutralize toxic compounds such as lipid peroxidation products and prostaglandins, contributing to the overall maintenance of cellular health and homeostasis.

In the present study, to gain a comprehensive understanding of the molecular signature underlying CRC progression, a cohort of patients representing diverse stages of colorectal diseases was assembled, aiming to map the progression from normal colonic epithelium to adenomatous lesions and invasive carcinoma. Using RNA-sequencing (RNA-seq) analysis of clinical samples, the present study systematically identified and characterized differentially expressed genes (DEGs) in CRC, providing a comprehensive gene expression profile. The glutathione metabolic pathway is crucial for maintaining cellular homeostasis and preventing oncogenic transformation. Key components of this pathway include microsomal glutathione S-transferase 3 (*MGST3*), peroxiredoxin 6 (*PRDX6*), hematopoietic prostaglandin D synthase (*HPGDS*), γ-glutamyltransferase 1 (*GGT1*), glutathione peroxidase 3 (*GPX3*), glutathione S-transferase μ4 (*GSTM4*), glutathione S-transferase α1 (*GSTA1*) and glutathione reductase (*GSR*). Therefore, the present study aimed to investigate the functional role of *MGST3* in colon carcinogenesis, with a specific focus on its potential link to ferroptosis. To achieve this, short hairpin RNA (shRNA) was employed to knock down *MGST3* expression in cell models and the resulting susceptibility to ferroptosis was assessed. These discoveries may provide insights into the molecular mechanisms of CRC, particularly colon cancer, and highlight the potential of *MGST3* and related genes as biomarkers for early detection and as therapeutic targets. By targeting these pathways, novel strategies for CRC prevention and treatment can be developed, ultimately improving patient outcomes.

Materials and methods

Clinical samples. A retrospective analysis was performed on samples from patients with colorectal tumors treated at the Department of Gastroenterology, The Seventh Medical Center of Chinese PLA General Hospital (Beijing, China) between October 1, 2016 and October 31, 2016. Patient selection was based on the following inclusion criteria: i) Pathological confirmation of colorectal adenoma or adenocarcinoma; ii) availability of fresh-frozen tumor tissue with paired adjacent normal tissue (within 5 cm of the tumor margin); and iii) complete clinical and pathological data. The exclusion criteria were: i) Prior neoadjuvant chemotherapy or radiotherapy; and ii) diagnosis of synchronous multiple cancers or hereditary CRC syndromes. Based on these criteria, a total of 10 patients were included. The cohort comprised 2 cases of tubular adenoma, 3 of villous adenoma, 3 with early-stage cancer and 2 with advanced tumors. In addition, 4 adjacent normal tissue samples from these 10 patients were collected as controls.

Cell culture. The normal human colon cell line NCM460 (cat. no. IM-H445; cell batch, IM-H445031603) was purchased from the Xiamen Yimo Biotechnology Co, Ltd. These cells were cultured in Dulbecco's Modified Eagle's Medium (DMEM; Procell Life Science & Technology Co., Ltd.) and supplemented with 10% (v/v) heat-inactivated fetal bovine serum (FBS; Shanghai ExCell Biology, Inc.), 1% (v/v) penicillin-streptomycin and 1% (v/v) L-glutamine. All cell lines were maintained in a humidified incubator at 37˚C with 5% CO_2. All cell lines tested negative for mycoplasma contamination.

Plasmid construction. To construct shRNA-expressing vectors, annealed complementary shRNA oligonucleotides were ligated into the PiggyBac-H1-2O2-shRNA-CopGFP-puro vector, which was constructed from the PiggyBac-CMV-CNR (human)-EF1a-CopGFP-T2A-Puro plasmid (cat. no. P31653; MiaoLingBio) by replacing the CMV promoter with the H1-2O2 promoter. The shRNA sequence was 5'-GCAAGAAGTACAAAGTGGAGT-3' and the sequence for the negative control group was 5'-TTCTCCGAACGTGTCACGT-3'. NCM460 cells were seeded into 6-well plates and transfected with a total of 4 μg of plasmid DNA using Lipofectamine 3000 reagent (cat. no. L3000008; Invitrogen; Thermo Fisher Scientific, Inc.). The plasmid mixture consisted of the shRNA-expressing PiggyBac vector and Super PiggyBac Transposase (cat. no. P0179; MiaoLingBio) at a mass ratio of 2.5:1. The DNA-lipid complexes were incubated at room temperature for 15 min before being added to the cells. After 24 h of incubation, the cells were selected with 1 μg/ml puromycin for 3 days, after which almost all surviving cells exhibited green fluorescence. Single clones were then obtained by serial dilution and maintained under a lower dose of puromycin (0.1 μg/ml) for 1 to 2 weeks to establish stable cell lines. Protein knockdown was finally confirmed by western blotting.

Clinical sample RNA-seq. RNA was extracted from clinical samples using RNAiso Plus (cat. no. 9109; Takara Bio, Inc.). The integrity of the RNA samples was assessed by agarose gel electrophoresis. RNA concentrations were quantified using a Qubit fluorometer (Thermo Fisher Scientific, Inc.) according to the manufacturer's instructions. Subsequent RNA-seq library preparation and deep sequencing were performed by BGI Genomics (Shenzhen, China). The samples were subjected to paired-end (2x150 bp) sequencing on an Illumina NovaSeq 6000 platform (cat. no. 20012850; Illumina, Inc.). Sequencing data were trimmed using Trimmomatic (v.0.39) (7) and aligned to the reference genome hg38 using STAR (v.2.7.7a) (8) software. Subsequently, read counting and differential gene expression analysis were performed using Cufflinks (v.2.2.1) (9). The data generated from the present study have been deposited in the NCBI Gene Expression Omnibus database under the accession number GSE316039.

Cell viability assays. Cell viability assays were performed as previously described (10). For cell viability assays, cells were seeded into 96-well plates ($1x10^3$/well) and then incubated

at 37˚C under 5% CO_2. The viability was measured at four different time points: 24, 48, 72 and 96 h. At each designated time point, 10 μl of Cell Counting Kit-8 (CCK-8) reagent (cat. no. HY-K0301; MedChemExpress) was added to each well, followed by incubation for an additional 2 h (the incubation duration was determined by a pre-experimental optimization to ensure the OD values were within the linear range). The optical density was then measured using a microplate spectrophotometer (BioTek Synergy H1; Agilent Technologies, Inc.).

Colony formation assay. The colony formation assay was performed as previously described (11). A total of $1x10^3$ shMGST3 and shNC transfected cells were seeded into 6-well plates. After 14 days, colonies were fixed with 4% paraformaldehyde (room temperature, 30 min), stained with 0.1% crystal violet (room temperature, 20 min) and imaged. Colonies containing ≥50 cells were quantified.

Scratch healing assay. The scratch healing assay was performed to assess the migration capacity of cells *in vitro* (12). Cells were seeded in 6-well plates and cultured in medium containing 3% FBS. A scratch was created across the monolayer using a 200 μl pipette tip. Cell migration was observed at 0 and 12 h post-scratch using a fluorescence microscope (magnification, x4) to monitor wound closure. Images were captured to evaluate the migration levels of the transfected cell groups. The wound healing rate was calculated using the formula: Percentage change=([width at 0 h - width at 12 h]/width at 0 h) x100.

Transwell assay. The Transwell assay was performed as previously described (13). The Transwell chamber contains a porous membrane with a pore size of 8 μm. To assess invasion capability, the bottom membrane of the chamber was coated with Matrigel at a ratio of 1:40 (Matrigel: serum-free medium; 100 μl). The lower chamber was filled with 500 μl of serum-free medium. The plates were then incubated at 37˚C for 2 h to allow the Matrigel to solidify. After 2 h, $5x10^4$ cells transfected with shMGST3 or shNC were seeded into the upper chamber, while the lower chamber was supplemented with 500 μl of DMEM containing 10% FBS. After a 24 h incubation at 37˚C in a 5% CO_2 incubator, cells on the membrane were fixed with 4% paraformaldehyde for 30 min at 25˚C, followed by staining with 0.1% crystal violet at 25˚C for 10 min. Following three PBS washes, non-migrated cells on the upper side of the membrane were removed with a cotton swab. In total, five random fields (magnification, x20) were selected under a fluorescence microscope using the brightfield mode and the number of stained cells was counted to quantify invasion.

Protein extraction and western blotting analysis. Protein extraction and western blotting assays were performed as previously described (14). Cells were lysed on ice using RIPA buffer (cat. no. 9806; Cell Signaling Technology, Inc.) supplemented with PMSF and protease inhibitors. The supernatant was collected and boiled for 10 min after adding 5x SDS protein loading Buffer (cat. no. 30215ES; Shanghai Yeasen Biotechnology Co., Ltd.). A total of 10 μg of protein per lane was resolved on 4-20% SDS-PAGE gels (cat. no. ET12420Gel; ACE Biotechnology Co., Ltd.) and subsequently transferred to a PVDF membrane (cat. no. ISEQ00010; MilliporeSigma). The membrane was blocked with 5% skim milk at room temperature for 1 h, followed by overnight incubation at 4˚C with primary antibodies against MGST3 (cat. no. ab192254; Abcam) and GAPDH (cat. no. GB15002-100; Wuhan Servicebio Technology Co., Ltd.) diluted to 1:1,000. Following incubation with the primary antibody, the membrane was washed three times with TBST (containing 0.1% Triton X-100) and then incubated for 1 h at room temperature with horseradish peroxidase-conjugated goat anti-rabbit IgG (H+L) (cat. no. A0208; Beyotime Biotechnology) and goat anti-mouse IgG (H+L) (cat. no. A0216; Beyotime Biotechnology), each at a dilution of 1:5,000. After another three TBST washes, protein bands were visualized using an ultrasensitive ECL chemiluminescent substrate (cat. no. P0018FM; Beyotime Biotechnology) and imaged with a Tanon system equipped with Tanon Bio Imaging Analysis Software (version 1.0.0000; Tanon Science & Technology Co., Ltd.).

Colon cancer data sets. Clinical variables including tumor node metastasis staging and the corresponding gene expression matrices profiles of patients with colon adenocarcinoma (COAD) were downloaded from The Cancer Genome Atlas (TCGA) database (https://portal.gdc.cancer.gov).

Enrichment analysis. Enrichment analysis were conducted on Metascape (https://metascape.org/) with the following screening criteria: A minimum overlap of 3 genes, $P \leq 0.01$ and a minimum enrichment factor of 1.5. The signals of the 14 pathways in the high and low expression samples of the glutathione gene set were calculated using the PROGENy package (15) in R software (version 4.2.3; https://www.R-project.org/), with samples stratified into high- and low-expression groups based on the median expression of the glutathione gene set derived from TCGA colon cancer data.

Protein-protein interaction (PPI) molecular analysis. Search Tool for the Retrieval of Interacting Genes (https://cn.string-db.org) (16) was employed for constructing PPI networks using the gene set from Cluster 3. The resulting network file was imported into Cytoscape software (version 3.9.1) (17), which generated multiple subnetworks. The MCODE plugin (version 2.0.3) was applied to identify the most significant subnetwork based on the node score and number of genes, defined as a module with a node score >5 and containing >10 genes. Subsequently, the hub genes were selected from this subnetwork using the cytoHubba plugin (version 0.1).

Tumor mutation burden (TMB). TMB was defined as the total number of somatic coding base substitutions, insertions and deletions per megabase of examined genome (18). Using the TCGA-COAD cohort, stratified by the expression level of the glutathione gene set, TMB analysis and distribution of tumor mutation types were calculated by R package maftools (version 2.14.0) (19).

Computation of EMT score. The EMT gene sets in both the study by Tan *et al* (20) and the EMTome database (http://www.emtome.org) were searched and the enrichment scores of the samples with high and low expression of the glutathione

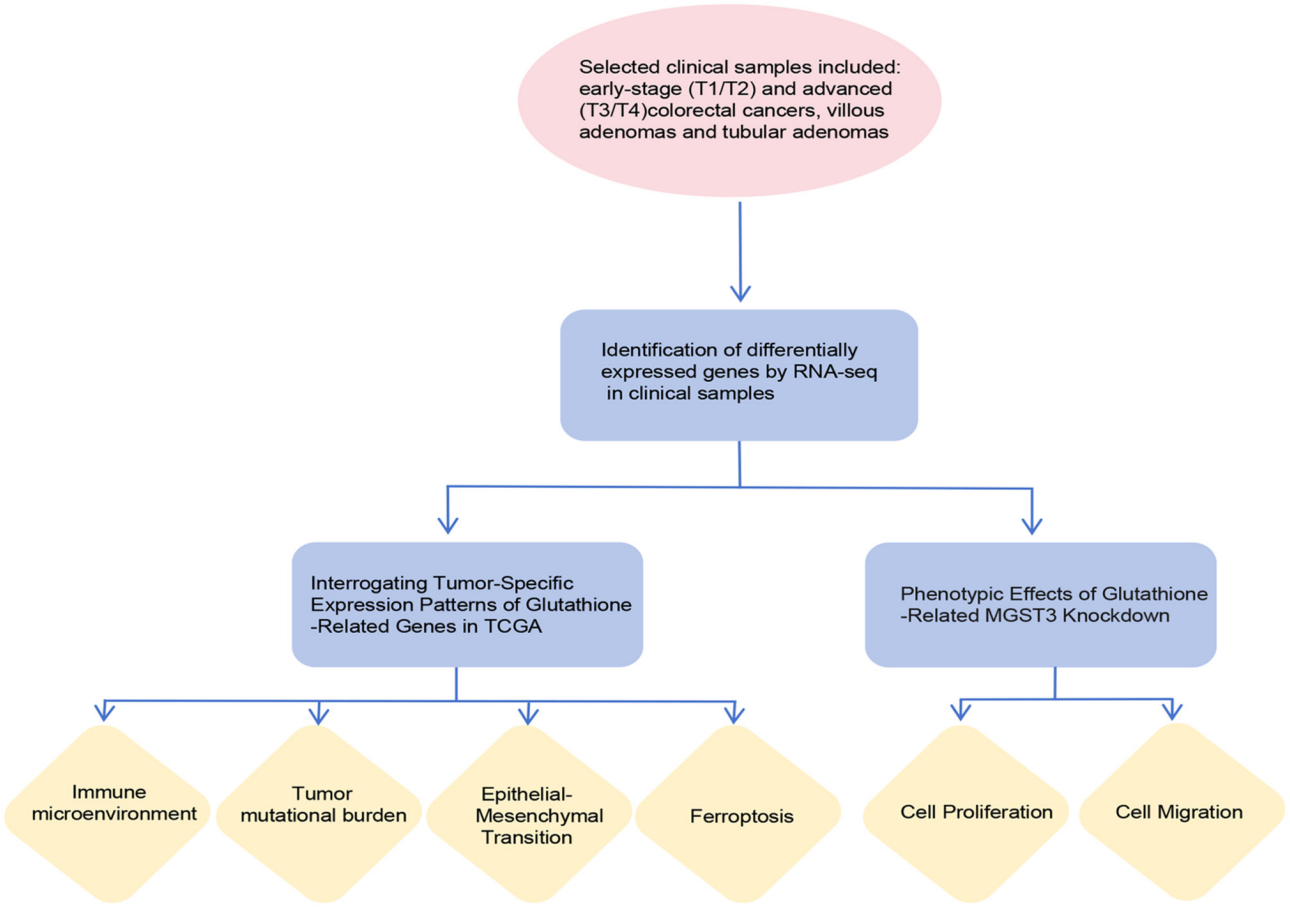

Figure 1. Schematic diagram of the experimental workflow. RNA-seq, RNA sequencing; TCGA, The Cancer Genome Atlas; MGST3, microsomal glutathione S-transferase 3.

gene set were calculated using the single-sample Gene Set Enrichment Analysis (GSEA) algorithm (21).

Tumor immune infiltration analysis. The tumor immune infiltration analysis was performed using the CIBERSORT (version 0.1.0) (22) and ESTIMATE packages (version 1.0.13) (23) within the R (version 4.2.3) programming environment and based on gene expression matrices obtain from TCGA database.

Statistical analyses. Statistical analyses were performed as follows: Fisher's exact test was used for Kyoto Encyclopedia of Genes and Genomes (KEGG) pathway enrichment analysis of DEGs from the RNA-seq data; gene expression across different tumor stages in TCGA database were analyzed by Kruskal-Wallis test followed by Dunn's multiple comparisons test; a two-tailed unpaired t-test was applied to analyze the following metrics: TMB, immune score and the results of the Transwell and scratch healing assays, comparison of ferroptosis-related gene expression and pathway signals (14 pathways) between samples stratified by high and low expression levels of the glutathione gene set; two-way ANOVA test followed by Bonferroni's multiple comparisons test was employed for proliferation analysis of shMGST3 and shNC cells; and the Kolmogorov-Smirnov test was used for GSEA of the glutathione gene set. $P<0.05$ was considered to indicate a statistically significant difference.

Results

Determination of a gene cluster that has low expression in CRC. Colorectal tumor samples from 5 male and 5 female patients, all aged 40-60 years were classified into early-stage tumors (pathological T1/T2), advanced tumors (pathological T3/T4), villous adenomas and tubular adenomas. This analytical approach included RNA-seq of patient samples, functional phenotypic validation in cell models and bioinformatics analyses of tumor-related indicators using data from TCGA database (TCGA-COAD cohort) (Fig. 1). Specifically, differential gene expression analysis [$P<0.01$, $|\log_2(\text{fold change})| \geq 1$] was performed comparing adjacent normal tissues to the defined tumor stages (Fig. 2A). Through clustering of significant DEGs, four distinct expression patterns were identified: i) Cluster 1 (601 genes) showed specific upregulation in advanced tumors; ii) Cluster 2 (482 genes) exhibited high expression in normal tissues but progressive downregulation across precancerous lesions (villous/tubular adenomas) and tumors, with maximal suppression in advanced cases; iii) Cluster 3 (574 genes) demonstrated elevated expression in normal tissues that sharply declined in tubular adenomas and showed further reduction in villous adenomas and tumors; and iv) Cluster 4 (447 genes) displayed consistently lower expression in normal tissues vs. all pathological groups.

Among these clusters, Cluster 3 exhibited the most uniform and distinct expression patterns in CRC, differing markedly

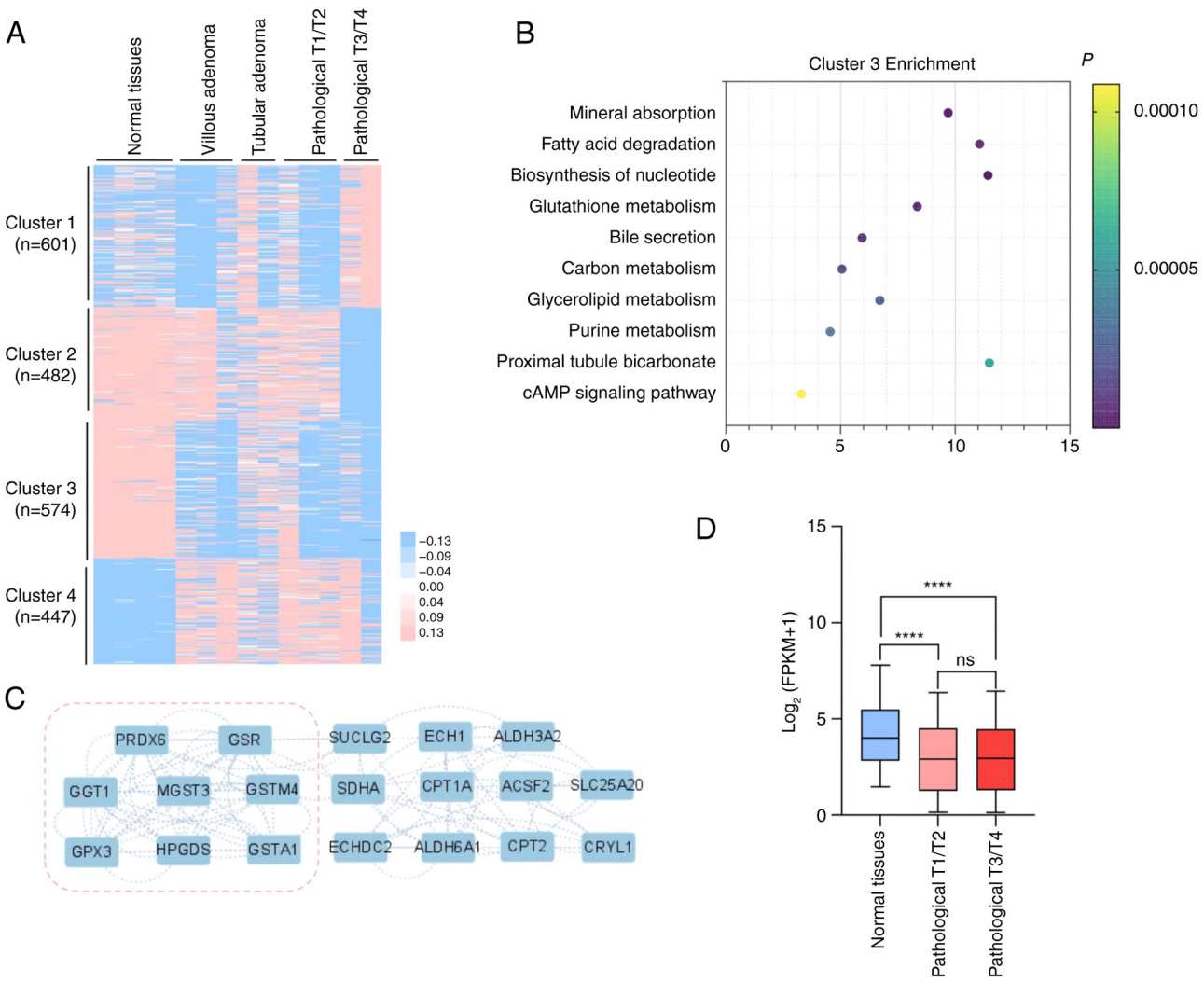

Figure 2. Discovering a gene cluster that has low expression in colorectal cancer. (A) Four types of clustering analysis of differentially expressed genes between different tumors: Adjacent normal tissues (n=4), villous adenoma (n=3), tubular adenoma (n=2), pathological T1/T2 (n=3) and pathological T3/T4 (n=2). (B) The top 10 pathways enriched by Kyoto Encyclopedia of Genes and Genomes clustering analysis of the Cluster 3 genes. (Fisher's exact test). (C) The molecular interaction network with the most genes in Cluster 3. The genes within the pink dashed box represents those enriched in the glutathione pathway. (D) Differential analysis of normal, pathological T1/T2 tumor and pathological T3/T4 tumor tissues according to TCGA database (TCGA-COAD cohort). Data were analyzed using Kruskal-Wallis test followed by Dunn's multiple comparisons test; ****P<0.0001. ns, not significant; FPKM, fragments per kilobase of exon model per million mapped fragments; TCGA, The Cancer Genome Atlas; COAD, colon adenocarcinoma.

from both adjacent normal tissues and adenomas. Given this clear differentiation, Cluster 3 was selected for further investigation. KEGG pathway enrichment analysis revealed that the top enriched pathways in this cluster were predominantly metabolic-related (Fig. 2B). PPI network analysis using Cytoscape identified the 'Glutathione metabolism' pathway as containing the highest proportion of hub genes (Fig. 2C), suggesting its potential central role in CRC pathogenesis. Glutathione metabolism has been functionally implicated in CRC pathogenesis (24). Based on this network analysis, a glutathione metabolism gene set comprising eight key enzymes: *MGST3*, *PRDX6*, *HPGDS*, *GGT1*, *GPX3*, *GSTM4*, *GSTA1* and *GSR* was identified. These genes were selected based on their hub status in the PPI network and their enrichment in glutathione-related pathways.

To validate these findings, transcriptomic data from TCGA-COAD were analyzed, stratifying the samples by clinical stage (early and advanced tumors). The glutathione gene set showed significantly higher expression in adjacent normal tissues compared with both tumor stages (Fig. 2D). This consistent downregulation across tumor progression suggests that glutathione pathway dysregulation may contribute to colon carcinogenesis. To further investigate the significance of the glutathione gene set, its expression patterns were analyzed across multiple malignancies. Consistently, reduced expression in tumor vs. normal adjacent tissue was observed in several tumor types, including breast invasive carcinoma, lung squamous cell carcinoma and stomach adenocarcinoma (Fig. S1). These findings were consistent with existing literature reports (25-29) and collectively demonstrated that glutathione pathway downregulation represents an early and conserved event in tumorigenesis across diverse cancer types, including CRC.

Differences in tumor characteristics and the immune microenvironment in the glutathione gene set. Given the established

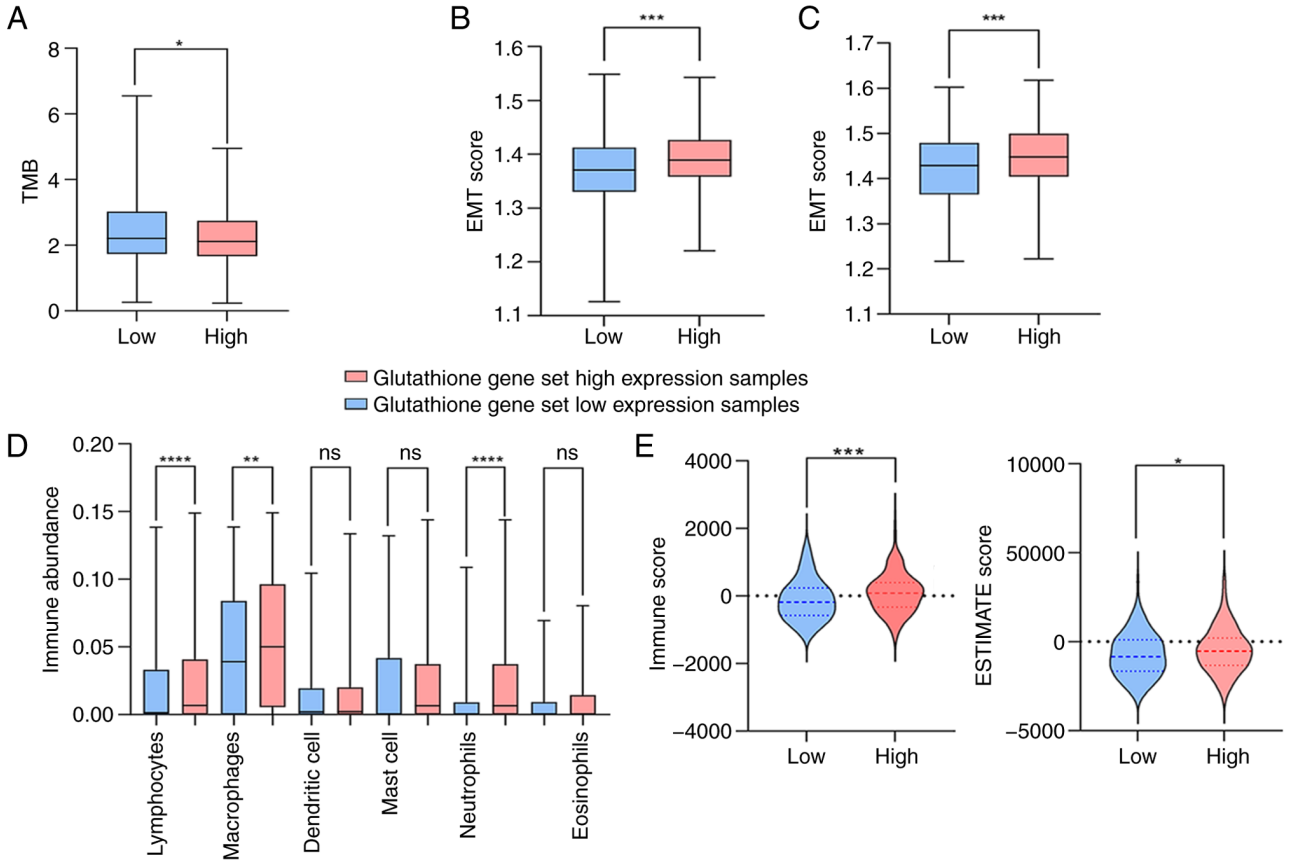

Figure 3. Differences in tumor characteristics and the immune microenvironment in glutathione gene set expression profiles in The Cancer Genome Atlas-colon adenocarcinoma cohort. (A) Differences in TMB between the high (n=178) and low (n=179) glutathione gene set expression samples (two-tailed unpaired t-test; *P<0.05). (B) Distribution of high and low glutathione gene set expression across lymphocyte, macrophage, dendritic cell, mast cell, neutrophil and eosinophil populations (two-tailed unpaired t-test; ns, not significant; **P<0.01, ****P<0.0001). (C) Difference in the EMT scores (gene set: EMTome) between the high (n=236) and low (n=235) glutathione gene set expression samples (two-tailed unpaired t-test; ***P<0.001). (D) EMT scores [gene set: Tan *et al* (20)] between high (n=236) and low (n=235) glutathione gene set expression samples (two-tailed unpaired t-test; ns, not significant; **P<0.01, ****P<0.0001). (E) Differences in immune score, estimate comprehensive score and stromal score between the high (n=236) and low (n=235) glutathione gene set expression samples. (two-tailed unpaired t-test; *P<0.05, ***P<0.001). EMT, epithelial-mesenchymal transition; TMB, tumor mutation burden.

interplay between CRC progression and the tumor microenvironment (TME) (30), the potential role of the glutathione gene set was investigated in this context. Using TCGA-COAD data, the expression profiles of these genes were extracted and their mean expression levels in each sample were calculated. Samples were then stratified into high and low expression groups based on median gene set expression, enabling comparative analysis of some characteristics between these subgroups. Next, differences in TMB, EMT markers (31) and immune cell infiltration (32) between the high and low expression groups were evaluated. Notably, it was found that tumors with low expression of the glutathione gene set exhibited significantly elevated TMB compared with tumors with high expression (Fig. 3A). Conversely, tumors with high expression showed significantly enhanced EMT activity (Fig. 3B and C). These results indicated that elevated expression of glutathione pathway genes may be associated with tumor aggressiveness, as previously reported (33).

To characterize the tumor immune microenvironment, immune cell infiltration profiling was performed using CIBERSORT. Infiltrating immune cells were characterized into six functional groups, including lymphocytes, macrophages, dendritic cells, mast cells, eosinophils and neutrophils, using the method described by Wellenstein and de Visser (34). Comparative analysis revealed significantly elevated infiltration of lymphocytes, macrophages and neutrophils in tumors with high expression of the glutathione gene set (Fig. 3D). These findings were validated using the ESTIMATE package, which similarly demonstrated enhanced overall immune activity in tumors with high expression (Fig. 3E). Collectively, these results demonstrated that elevated glutathione pathway activity may be associated with a more immunologically active TME, suggesting these genes may serve as potential biomarkers for immunotherapy response (35).

Knockdown of MGST3 promotes cell proliferation and migration. Within the glutathione-related genes, decreased *MGST3* expression may contribute to compromised carcinogen detoxification processes and further facilitate cellular transformation into a malignant state (36). To elucidate the functional consequences of MGST3 dysregulation in CRC, with a specific focus on colon carcinogenesis, stable MGST3 knockdown was established in the NCM460 normal human colon mucosal epithelial cell line (37). Western blot analysis confirmed efficient MGST3 depletion (Fig. 4A). Subsequent functional characterization revealed that shMGST3 transfection significantly enhanced

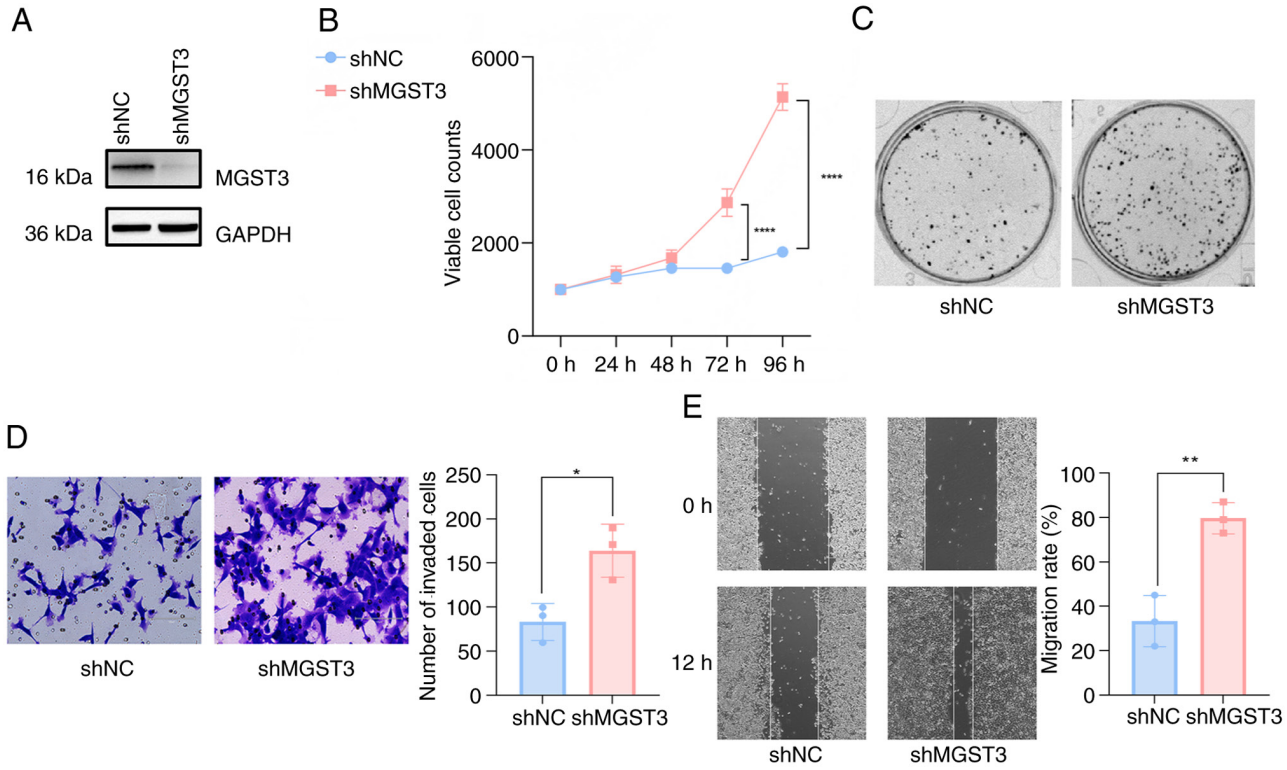

Figure 4. Knockdown of MGST3 promotes cell proliferation and migration. (A) Protein expression levels were assessed in NCM460 cell lines following knockdown with shMGST3 or shNC. (B) Proliferation analysis of shMGST3 and shNC cells. Top: Cell Counting Kit-8 assay (two-way ANOVA followed by Bonferroni's multiple comparisons test; ****P<0.0001). (C) Proliferation analysis of shMGST3 and shNC cells: Colony formation assay. (D) Migration analysis of shMGST3 and shNC cells: Transwell assay (magnification, x20). (E) Migration analysis of shMGST3 and shNC cells: Scratch healing assay (magnification, x4). Two-tailed unpaired t-test; *P<0.05, **P<0.01. MGST3, microsomal glutathione S-transferase 3; sh, short hairpin RNA; NC, negative control.

cellular proliferation compared with shNC, as demonstrated by both CCK-8 viability and colony formation assays (Fig. 4B). These results indicated that MGST3 deficiency promoted proliferative advantages in colonic epithelial cells, potentially representing an early event in malignant transformation.

To further evaluate the malignant potential conferred by MGST3 depletion, the invasive and migratory capacities were assessed. MGST3-knockdown cells demonstrated a significantly increased invasion and migration rate in compared with the shNC cells (Fig. 4D and E). These functional assays collectively established that knocking down MGST3 expression enhanced both the invasive and migratory properties of colon epithelial cells.

Relationship between MGST3 dysfunction and ferroptosis. Given the established connection between glutathione metabolism and ferroptosis regulation (38), key ferroptosis-associated genes in CRC (glutathione peroxidase 4, heat shock protein B1; solute carrier family 40 member 1 and lipocalin 2) were investigated (39-42). Comparative analysis revealed significantly reduced expression of these ferroptosis regulators in tumors with low expression of the glutathione gene set compared with tumors with high expression of the glutathione gene set (Fig. 5A). This consistent downregulation of key ferroptosis inhibitors suggests enhanced susceptibility to ferroptosis in tumors with lower expression of the glutathione gene set. Given that ferroptosis is closely related to the levels of reactive oxygen species (ROS) and fatty acid metabolism, GSEA was performed to systematically evaluate these pathways in the expression groups. Analysis of the glutathione gene set revealed a significantly stronger enrichment of both ROS-related and fatty acid metabolic gene signatures in the low expression group compared with the high expression group.(Fig. 5B and C). These results demonstrated that reduced glutathione pathway activity may be associated with molecular profiles characteristic of ferroptosis susceptibility, marked by enhanced ROS production and dysregulated lipid metabolism. Furthermore, analysis revealed a significant enrichment of the p53 pathway in samples where the glutathione gene set was highly expressed compared with samples with low expression (Fig. S2).

These integrated analyses demonstrated that elevated glutathione gene set expression confers resistance to ferroptosis in colon cancer cells, which potentially implies a more unfavorable prognosis for patients. This effect, potentially mediated through fatty acid metabolism and ROS regulation, suggests that glutathione gene set expression may serve as a potential therapeutic target.

Discussion

In the present study, gene expression analysis of patients with CRC, particularly in the colon, revealed a specific role for *MGST3* in the early phases of tumor development. While *MGST3* expression was significantly reduced in early-stage tumors compared with normal tissue, its expression levels remained stable across different stages of progression. This indicates that the reduction in MGST3 levels is a key early

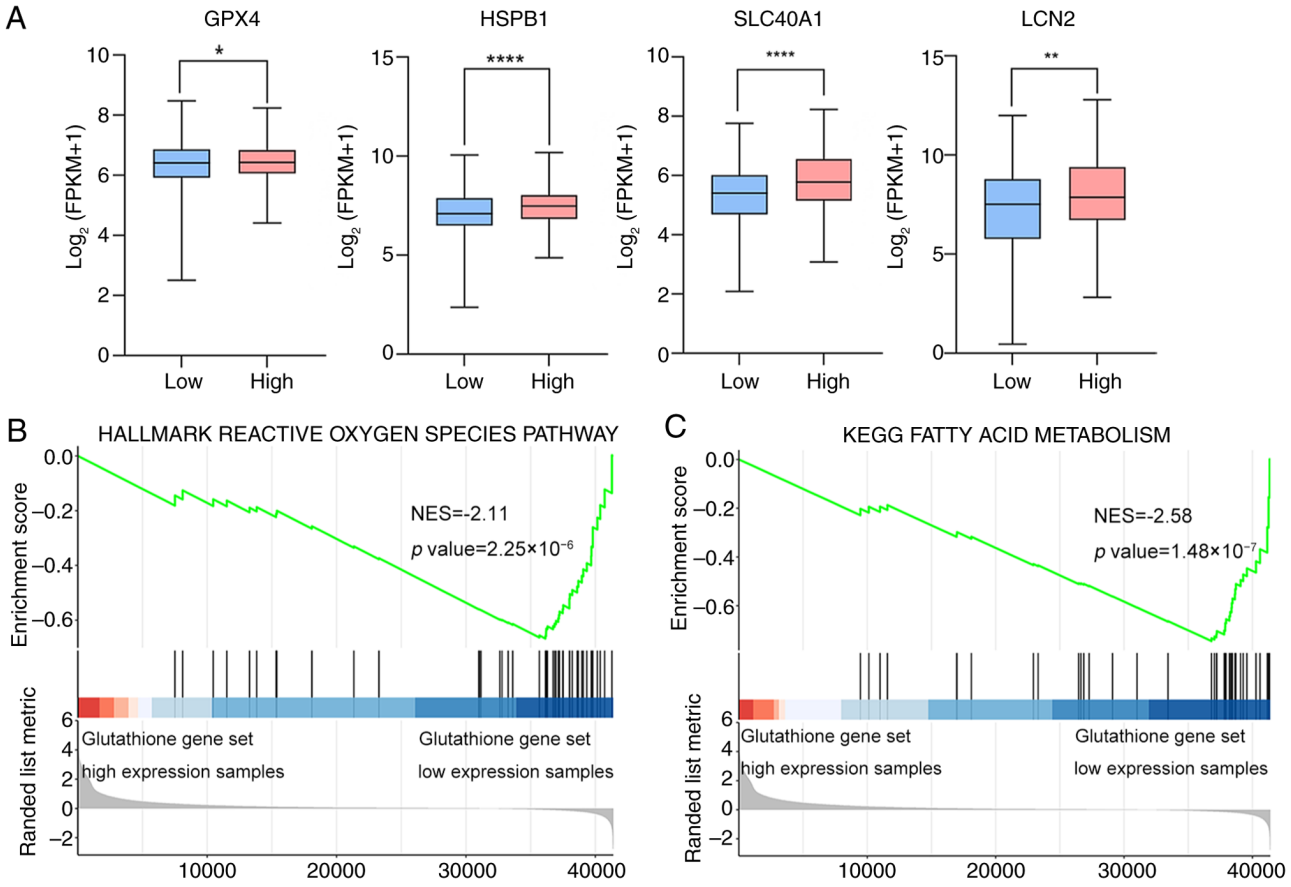

Figure 5. Relationship between the glutathione gene set dysfunction and ferroptosis. (A) The expression differences of ferroptosis-related genes in the glutathione gene set between the low (n=235) and high (n=236) expression samples in TCGA database (TCGA-COAD cohort) (two-tailed unpaired t-test; *P<0.05, **P<0.01, ****P<0.0001). (B) The enrichment status of the glutathione gene set between the low (n=235) and high (n=236) expression samples in the reactive oxygen species-related gene set by GSEA analysis. (C) The enrichment status of the glutathione gene set between the low (n=235) and high (n=236) expression samples in the fatty acid metabolism gene set by GSEA analysis (Kolmogorov-Smirnov test). FPKM, fragments per kilobase of exon model per million mapped fragments; GPX4, glutathione peroxidase 4; HSPB1, heat shock protein family B (small) member 1; SLC40A1, solute carrier family 40 member 1; LCN2, lipocalin-2; GSEA, Gene Set Enrichment Analysis; NES, normalized enrichment score; KEGG, Kyoto Encyclopedia of Genes and Genomes; TCGA, The Cancer Genome Atlas; COAD, colon adenocarcinoma.

event in the adenoma-carcinoma pathway, rather than a factor involved in the ongoing progression of the disease. This suggests that the loss of MGST3 function is a key driver of early colorectal tumorigenesis. Therefore, MGST3 not only represents a promising tumor suppressor but also a potential biomarker for the early detection of colon cancer specifically.

In the present study, based on PPI network analysis of DEGs, a highly interconnected core functional module and selected hub genes including *MGST3*, *PRDX6*, *HPGDS*, *GGT1*, *GPX3*, *GSTM4*, *GSTA1* and *GSR* were identified. These genes are primarily involved in glutathione metabolism and oxidative stress pathways. Notably, *MGST3*, *GSTM4* and *GSTA1* belong to the GST family, which comprises detoxifying enzymes that conjugate glutathione to mitigate oxidative damage from ROS and neutralize toxic compounds such as lipid peroxidation products, thereby maintaining cellular homeostasis and influencing colorectal tumor development (43). Other hub genes also play significant roles in tumor biology. For example, targeting GGT1 can alleviate immunosuppressive functions (44). Targeting GPX3, a key player in cholesterol-mediated T-cell immune responses in CRC, could be a viable strategy (45). Conversely, inhibiting PRDX6 expression diminishes the malignant potential of colon cancer cells (46). In summary, the identified hub genes are closely associated with key tumor-related pathways and processes, underscoring their importance in tumor progression.

In the present study these genes were termed the glutathione gene set. Considering the differences in their expression profiles in tumor samples, the present study focused on alterations in TMB, immune invasion and EMT in this gene cluster. The findings revealed that tumors with low expression of this gene cluster exhibited significantly lower TMB compared with those with high expression. In colon cancer, patients with increased TMB tend to have favorable prognoses. Additionally, numerous studies suggest that TMB can serve as a tumor biomarker (47-50) that can be used to identify patients who are most likely to respond to immune checkpoint inhibitors (ICIs). Therefore, patients with colon cancer who exhibit high expression of the glutathione gene set may be more suitable for ICI therapy (51).

Furthermore, in the present study, samples with high expression of the glutathione gene set demonstrated significantly higher EMT scores and immune infiltration levels of lymphocytes, macrophages and neutrophils compared with those with low expression. Originally described during

embryonic development, EMT involves the transformation of epithelial cells into cells with a mesenchymal phenotype (52). This process not only enhances the motility and invasiveness of cancer cells but also enables them to evade apoptosis, oncogene addiction, cellular senescence and general immune defense mechanisms (53). Therefore, EMT is an integral component of colon cancer progression and its analysis can provide novel targets for prognosis and therapy. The number and types of tumor-infiltrating immune cells have been proven to be crucial indicators of effective antitumor immune responses, ultimately determining the prognosis of cancer (54). Additionally, tumor-associated macrophages and neutrophils have been strongly associated with poor prognosis in patients with CRC (55). Based on these observations, we consider that patients with higher expression of this gene cluster may be more prone to tumor metastasis and have a less favorable prognosis.

A previous study has indicated a close association between glutathione redox status and the progression of CRC, where the induction of glutathione synthesis has been shown to promote liver metastasis of CRC (56). The present study showed that colon cancer samples with low expression of the glutathione gene set were significantly enriched in ROS response and fatty acid metabolism-related gene sets compared with those with high expression of the glutathione gene set. Research has shown that ROS are involved in lipid peroxidation. Specifically, this process generates compounds such as 4-hydroxynonenal and the peroxidation of the phospholipid bilayer may facilitate the occurrence of ferroptosis (57). This suggests that colon cancer with low expression of the glutathione gene set is more prone to ferroptosis than colon cancer with high expression. Typically, tumors experiencing ferroptosis exhibit a more favorable prognosis (58).

In the present study, a significant enrichment of the p53 pathway was observed in samples with high expression of the glutathione gene set compared with those with low expression. Upon activation, p53 can mediate a diverse array of cellular responses, encompassing ferroptosis, stem cell reprogramming, invasion and metastasis as well as metabolic regulation (59). p53 inhibits dipeptidyl peptidase 4 (DPP4) activity and negatively regulates ferroptosis in CRC cells. Conversely, the absence of p53 promotes the interaction between DPP4 and NADPH oxidase 1 (NOX1), leading to the formation of a NOX1-DPP4 complex that mediates plasma membrane lipid peroxidation and subsequently triggers ferroptosis (60). Therefore, in samples with low expression of the glutathione gene set, the inhibition of p53 may be responsible for the induction of ferroptosis. Meanwhile, in drug treatments targeting tumors with a high expression profile of the glutathione gene set, modulation of ferroptosis occurrence through targeting p53, as primarily investigated in colon cancer models, may hold notable implications for the progression of CRC, offering significance for targeted therapies in CRC (61). The present study identified changes and influences of *MGST3* and a set of genes (including *PRDX6, HPGDS, GGT1, GPX3, GSTM4, GSTA1* and *GSR*) whose products interact within a PPI network in the occurrence and progression of CRC, adding a significant contribution to the research and treatment of CRC.

In the present study, although the knockdown experiments demonstrated that MGST3 deficiency activated glutathione metabolism and induces tumorigenic phenotypes, the precise molecular mechanisms by which MGST3 may regulate this pathway, such as through specific protein interactions or transcriptional regulation, remain incompletely elucidated. Furthermore, the present study did not include overexpression experiments or *in vivo* animal model validation, which limits the generalizability of the potential tumor-suppressive function of MGST3. In addition, while low MGST3 expression was associated with increased TMB, altered immune infiltration, suppressed EMT and enhanced ferroptosis, the causal relationships among these phenotypes have not been established. For instance, it remains unclear whether the potentiation of ferroptosis and the observed immunosuppressive microenvironment are directly linked or merely concurrent events. Finally, independent validation of the key findings in a separate cohort represents an essential future objective, as it fell beyond the scope and resources of the present study.

Acknowledgements

Not applicable.

Funding

This research was financially supported by the National Natural Science Foundation of China for Young Scholars (grant no. 32100460).

Availability of data and materials

The RNA-seq data generated in the present study may be found in the NCBI Gene Expression Omnibus database under the accession number GSE316039 or at the following URL: https://www.ncbi.nlm.nih.gov/geo/query/acc.cgi?acc=GSE316039.

Authors' contributions

YW was responsible for the original concept, data collection, figure creation, experimental design and writing the manuscript. CF and FH contributed to data collection and the acquisition of research materials. JZ and YZ made substantial contributions to the conception and design of the study and performed critical revision of the manuscript for important intellectual content. JW and YH were responsible for the analysis and interpretation of data and provided project supervision. All authors read and approved the final version of the manuscript. YW and JW confirm the authenticity of all the raw data.

Ethics approval and consent to participate

This study was performed in line with the principles of the Declaration of Helsinki. Approval was granted by the Ethics Committee of the Chinese People's Liberation Army General Hospital (approval no. 2016-70). Informed consent for participation in the study was obtained from all patients. Additionally, separate consent was obtained for the publication of the data.

Patient consent for publication

Not applicable.

Competing interests

The authors declare that they have no competing interests.

Use of artificial intelligence tools

During the preparation of this work, artificial intelligence tools were used to improve the readability and language of the manuscript or to generate images, and subsequently, the authors revised and edited the content produced by the artificial intelligence tools as necessary, taking full responsibility for the ultimate content of the present manuscript.

References

1. Siegel RL, Giaquinto AN and Jemal A: Cancer statistics, 2024. CA Cancer J Clin 74: 12-49, 2024.
2. Qu R, Ma Y, Zhang Z and Fu W: Increasing burden of colorectal cancer in China. Lancet Gastroenterol Hepatol 7: 700, 2022.
3. Dantas AAG, de Oliveira NPD, Costa GAB, Martins LFL, Dos Santos JEM, Migowski A, de Camargo Cancela M and de Souza DLB: Multilevel analysis of social determinants of advanced stage colorectal cancer diagnosis. Sci Rep 14: 9667, 2024.
4. Myers DJ and Arora K: Villous adenoma (Archived). In: StatPearls. StatPearls Publishing, Treasure Island, FL, 2025.
5. Nguyen LH, Goel A and Chung DC: Pathways of colorectal carcinogenesis. Gastroenterology 158: 291-302, 2020.
6. Uno Y, Murayama N, Kunori M and Yamazaki H: Characterization of microsomal glutathione S-transferases MGST1, MGST2, and MGST3 in cynomolgus macaque. Drug Metab Dispos 41: 1621-1625, 2013.
7. Bolger AM, Lohse M and Usadel B: Trimmomatic: A flexible trimmer for Illumina sequence data. Bioinformatics 30: 2114-2120, 2014.
8. Dobin A, Davis CA, Schlesinger F, Drenkow J, Zaleski C, Jha S, Batut P, Chaisson M and Gingeras TR: STAR: Ultrafast universal RNA-seq aligner. Bioinformatics 29: 15-21, 2013.
9. Ghosh S and Chan CK: Analysis of RNA-seq data using tophat and cufflinks. Methods Mol Biol 1374: 339-361, 2016.
10. Adan A, Kiraz Y and Baran Y: Cell proliferation and cytotoxicity assays. Curr Pharm Biotechnol 17: 1213-1221, 2016.
11. Franken NA, Rodermond HM, Stap J, Haveman J and van Bree C: Clonogenic assay of cells in vitro. Nat Protoc 1: 2315-2319, 2006.
12. Liang CC, Park AY and Guan JL: In vitro scratch assay: A convenient and inexpensive method for analysis of cell migration in vitro. Nat Protoc 2: 329-333, 2007.
13. Justus CR, Marie MA, Sanderlin EJ and Yang LV: Transwell in vitro cell migration and invasion assays. Methods Mol Biol 2644: 349-359, 2023.
14. Mahmood T and Yang PC: Western blot: Technique, theory, and trouble shooting. N Am J Med Sci 4: 429-434, 2012.
15. Schubert M, Klinger B, Klünemann M, Sieber A, Uhlitz F, Sauer S, Garnett MJ, Blüthgen N and Saez-Rodriguez J: Perturbation-response genes reveal signaling footprints in cancer gene expression. Nat Commun 9: 20, 2018.
16. Szklarczyk D, Nastou K, Koutrouli M, Kirsch R, Mehryary F, Hachilif R, Hu D, Peluso ME, Huang Q, Fang T, *et al*: The STRING database in 2025: protein networks with directionality of regulation. Nucleic Acids Res 53: D730-D737, 2025.
17. Shannon P, Markiel A, Ozier O, Baliga NS, Wang JT, Ramage D, Amin N, Schwikowski B and Ideker T: Cytoscape: A software environment for integrated models of biomolecular interaction networks. Genome Res 13: 2498-2504, 2003.
18. Guo X, Liang X, Wang Y, Cheng A, Zhang H, Qin C and Wang Z: Significance of tumor mutation burden combined with immune infiltrates in the progression and prognosis of advanced gastric cancer. Front Genet 12: 642608, 2021.
19. Mayakonda A, Lin DC, Assenov Y, Plass C and Koeffler HP: Maftools: Efficient and comprehensive analysis of somatic variants in cancer. Genome Res 28: 1747-1756, 2018.
20. Tan TZ, Miow QH, Miki Y, Noda T, Mori S, Huang RY and Thiery JP: Epithelial-mesenchymal transition spectrum quantification and its efficacy in deciphering survival and drug responses of cancer patients. EMBO Mol Med 6: 1279-1293, 2014.
21. Subramanian A, Tamayo P, Mootha VK, Mukherjee S, Ebert BL, Gillette MA, Paulovich A, Pomeroy SL, Golub TR, Lander ES and Mesirov JP: Gene set enrichment analysis: A knowledge-based approach for interpreting genome-wide expression profiles. Proc Natl Acad Sci USA 102: 15545-15550, 2005.
22. Chen B, Khodadoust MS, Liu CL, Newman AM and Alizadeh AA: Profiling tumor infiltrating immune cells with CIBERSORT. Methods Mol Biol 1711: 243-259, 2018.
23. Yoshihara K, Shahmoradgoli M, Martínez E, Vegesna R, Kim H, Torres-Garcia W, Treviño V, Shen H, Laird PW, Levine DA, *et al*: Inferring tumour purity and stromal and immune cell admixture from expression data. Nat Commun 4: 2612, 2013.
24. Yan H, Talty R and Johnson CH: Targeting ferroptosis to treat colorectal cancer. Trends Cell Biol 33: 185-188, 2023.
25. Jardim BV, Moschetta MG, Leonel C, Gelaleti GB, Regiani VR, Ferreira LC, Lopes JR and Zuccari DAPDC: Glutathione and glutathione peroxidase expression in breast cancer: An immunohistochemical and molecular study. Oncol Rep 30: 1119-1128, 2013.
26. Inoue T, Ishida T, Sugio K, Maehara Y and Sugimachi K: Glutathione S transferase Pi is a powerful indicator in chemotherapy of human lung squamous-cell carcinoma. Respiration 62: 223-227, 1995.
27. Xu H, Hu C, Wang Y, Shi Y, Yuan L, Xu J, Zhang Y, Chen J, Wei Q, Qin J, *et al*: Glutathione peroxidase 2 knockdown suppresses gastric cancer progression and metastasis via regulation of kynurenine metabolism. Oncogene 42: 1994-2006, 2023.
28. Xiao Y and Meierhofer D: Glutathione metabolism in renal cell carcinoma progression and implications for therapies. Int J Mol Sci 20: 3672, 2019.
29. Sobhakumari A, Love-Homan L, Fletcher EV, Martin SM, Parsons AD, Spitz DR, Knudson CM and Simons AL: Susceptibility of human head and neck cancer cells to combined inhibition of glutathione and thioredoxin metabolism. PLoS One 7: e48175, 2012.
30. Schmitt M and Greten FR: The inflammatory pathogenesis of colorectal cancer. Nat Rev Immunol 21: 653-667, 2021.
31. Kalluri R and Weinberg RA: The basics of epithelial-mesenchymal transition. J Clin Invest 119: 1420-1428, 2009.
32. Bethmann D, Feng Z and Fox BA: Immunoprofiling as a predictor of patient's response to cancer therapy-promises and challenges. Curr Opin Immunol 45: 60-72, 2017.
33. Tiwari N, Gheldof A, Tatari M and Christofori G: EMT as the ultimate survival mechanism of cancer cells. Semin Cancer Biol 22: 194-207, 2012.
34. Wellenstein MD and de Visser KE: Cancer-cell-intrinsic mechanisms shaping the tumor immune landscape. Immunity 48: 399-416, 2018.
35. Mukherjee AG, Wanjari UR, Namachivayam A, Murali R, Prabakaran DS, Ganesan R, Renu K, Dey A, Vellingiri B, Ramanathan G, *et al*: Role of immune cells and receptors in cancer treatment: An immunotherapeutic approach. Vaccines (Basel) 10: 1493, 2022.
36. Mazari AMA, Zhang L, Ye ZW, Zhang J, Tew KD and Townsend DM: The multifaceted role of glutathione S-transferases in health and disease. Biomolecules 13: 688, 2023.
37. Moyer MP, Manzano LA, Merriman RL, Stauffer JS and Tanzer LR: NCM460, a normal human colon mucosal epithelial cell line. In Vitro Cell Dev Biol Anim 32: 315-317, 1996.
38. Xue X, Wang M, Cui J, Yang M, Ma L, Kang R, Tang D and Wang J: Glutathione metabolism in ferroptosis and cancer therapy. Cancer Lett 621: 217697, 2025.
39. Ma T, Du J, Zhang Y, Wang Y, Wang B and Zhang T: GPX4-independent ferroptosis-a new strategy in disease's therapy. Cell Death Discov 8: 434, 2022.
40. Sun X, Ou Z, Xie M, Kang R, Fan Y, Niu X, Wang H, Cao L and Tang D: HSPB1 as a novel regulator of ferroptotic cancer cell death. Oncogene 34: 5617-5625, 2015.
41. Zhang Y, Zou L, Li X, Guo L, Hu B, Ye H and Liu Y: SLC40A1 in iron metabolism, ferroptosis, and disease: A review. WIREs Mech Dis 16: e1644, 2024.

42. Chaudhary N, Choudhary BS, Shah SG, Khapare N, Dwivedi N, Gaikwad A, Joshi N, Raichanna J, Basu S, Gurjar M, *et al*: Lipocalin 2 expression promotes tumor progression and therapy resistance by inhibiting ferroptosis in colorectal cancer. Int J Cancer 149: 1495-1511, 2021.
43. Klusek J, Głuszek S and Klusek J: GST gene polymorphisms and the risk of colorectal cancer development. Contemp Oncol (Pozn) 18: 219-221, 2014.
44. Xie Z, Kawasaki T, Zhou H, Okuzaki D, Okada N and Tachibana M: Targeting GGT1 eliminates the tumor-promoting effect and enhanced immunosuppressive function of myeloid-derived suppressor cells caused by G-CSF. Front Pharmacol 13: 873792, 2022.
45. Chen J, Wu Y, Zhou Q, Song Y, Zhuang J, Lu K and Yang X: GPX3 is a key cholesterol-related gene associated with prognosis and tumor-infiltrating T cells in colorectal cancer. Neoplasma 70: 230704N348, 2023.
46. Lagal DJ, Montes-Osuna AM, Ortiz-Olivencia A, Arribas-Parejas C, Ortiz-Alcántara Á, Pescuezo-Castillo C, Bárcena JA, Padilla CA and Requejo-Aguilar R: Tumoral malignancy decreases coupled with higher ROS and lipid peroxidation in HCT116 Colon cancer cells upon loss of PRDX6. Antioxidants (Basel) 13: 881, 2024.
47. Merino DM, McShane LM, Fabrizio D, Funari V, Chen SJ, White JR, Wenz P, Baden J, Barrett JC, Chaudhary R, *et al*: Establishing guidelines to harmonize tumor mutational burden (TMB): In silico assessment of variation in TMB quantification across diagnostic platforms: Phase I of the friends of cancer research TMB harmonization project. J ImmunoTher Cancer 8: e000147, 2020.
48. Sha D, Jin Z, Budczies J, Kluck K, Stenzinger A and Sinicrope FA: Tumor mutational burden as a predictive biomarker in solid tumors. Cancer Discov 10: 1808-1825, 2020.
49. Zgura A, Chipuc S, Bacalbasa N, Haineala B, Rodica A and Sebastian V: Evaluating tumour mutational burden as a key biomarker in personalized cancer immunotherapy: A Pan-cancer systematic review. *Cancers* (Basel) 17: 480, 2025.
50. Kim ES, Velcheti V, Mekhail T, Yun C, Shagan SM, Hu S, Chae YK, Leal TA, Dowell JE, Tsai ML, *et al*: Blood-based tumor mutational burden as a biomarker for atezolizumab in non-small cell lung cancer: The phase 2 B-F1RST trial. Nat Med 28: 939-945, 2022.
51. Addeo A, Friedlaender A, Banna GL and Weiss GJ: TMB or not TMB as a biomarker: That is the question. Crit Rev Oncol/Hematol 163: 103374, 2021.
52. Brabletz T, Kalluri R, Nieto MA and Weinberg RA: EMT in cancer. Nat Rev Cancer 18: 128-134, 2018.
53. Kim DH, Xing T, Yang Z, Dudek R, Lu Q and Chen YH: Epithelial mesenchymal transition in embryonic development, tissue repair and cancer: A comprehensive overview. J Clin Med 7: 1, 2017.
54. Atreya I and Neurath MF: Immune cells in colorectal cancer: Prognostic relevance and therapeutic strategies. Expert Rev Anticancer Ther 8: 561-572, 2008.
55. Ye L, Zhang T, Kang Z, Guo G, Sun Y, Lin K, Huang Q, Shi X, Ni Z, Ding N, *et al*: Tumor-infiltrating immune cells act as a marker for prognosis in colorectal cancer. Front Immunol 10: 2368, 2019.
56. Nguyen A, Loo JM, Mital R, Weinberg EM, Man FY, Zeng Z, Paty PB, Saltz L, Janjigian YY, de Stanchina E and Tavazoie SF: PKLR promotes colorectal cancer liver colonization through induction of glutathione synthesis. J Clin Investig 126: 681-694, 2016.
57. Endale HT, Tesfaye W and Mengstie TA: ROS induced lipid peroxidation and their role in ferroptosis. Front Cell Dev Biol 11: 1226044, 2023.
58. Li S, Tao K, Yun H, Yang J, Meng Y, Zhang F and Ma X: Ferroptosis is a protective factor for the prognosis of cancer patients: A systematic review and meta-analysis. BMC Cancer 24: 604, 2024.
59. Liebl MC and Hofmann TG: The role of p53 signaling in colorectal cancer. Cancers (Basel) 13: 2125, 2021.
60. Xie Y, Zhu S, Song X, Sun X, Fan Y, Liu J, Zhong M, Yuan H, Zhang L, Billiar TR, *et al*: The tumor suppressor p53 limits ferroptosis by blocking DPP4 activity. Cell Rep 20: 1692-1704, 2017.
61. Yang L, WenTao T, ZhiYuan Z, Qi L, YuXiang L, Peng Z, Ke L, XiaoNa J, YuZhi P, MeiLing J, *et al*: Cullin-9/p53 mediates HNRNPC degradation to inhibit erastin-induced ferroptosis and is blocked by MDM2 inhibition in colorectal cancer. Oncogene 41: 3210-3221, 2022.